EXPERIMENTAL AND NUMERICAL INVESTIGATION OF THERMAL AND FLUID FLOW PROCESSES IN A MATRIX HEAT EXCHANGER

Mladen A. TOMIĆ[a1], Predrag M. ŽIVKOVIĆ[b], Biljana B. MILUTINOVIĆ[a], Mića V. VUKIĆ[b] and Aleksandra D. BORIČIĆ[a]

[a] *The College of Applied Technical Sciences, Niš, Serbia*
[b] *The University of Niš, Faculty of Mechanical Engineering, Niš, Serbia*

The need for compact heat exchangers has led to the development of many types of surfaces that enhance the rate of heat transfer, among them the matrix heat exchangers. These heat exchangers consist of a series of perforated plates mutually separated and sealed by spacers. The goal of this research was to investigate the heat transfer process of matrix heat exchangers on the air side, at the close to ambient conditions. The research was conducted in two directions - experimental research and CFD research. The experimental investigation was carried out over a perforated plate package with the porosity of 25.6%. The air/water matrix heat exchanger was installed in an experimental chamber at which entrance was a fan with the variable flow rate and heated by hot water. The thermocouples were attached to the surface of the perforated plate at the upwind and downwind sides, as well as at the inlet and the outlet of the chamber. During each experiment, the thermocouple readings and the air and water flow and temperatures were recorded. In the numerical part of the research, the matrix heat exchangers with different plate porosity from 10 to 50% were investigated. The results of the numerical simulations were validated against the experimental results. On the basis of the experimental and numerical results, equations for heat transfer and pressure drops were established.

Keywords: *CFD, Heat transfer, Matrix heat exchangers*

1. Introduction

One of the most important properties of heat exchangers, a part of having a high effectiveness is the need to be very compact, *i.e.* they must accommodate a large surface to volume ratio. This helps in controlling the heat exchanger exposure to the surroundings by reducing the exposed surface area. A small mass means a smaller heat inertia. This requirement is particularly important for small refrigerators operating at liquid helium temperature. The need of attaining high effectiveness and a high level of compactness together in one unit led to the invention of matrix heat exchangers (MHE) by McMation *et al.* [1]. Matrix heat exchanger consists of a package of perforated plates with a multitude of flow passages aligned in the direction of flow, allowing high heat transfer in a proper design unit. This exchanger can have up to 6000 m^2/m^3 surfaces to volume ratio [2,3]. The development of matrix heat exchangers has largely been directed towards the use in helium liquefiers and, more recently, towards low power cryorefrigerators based on Claude' and reverse Brayton cycles [3].

[1] corresponding author e-mail: mladen.tomic@vtsnis.edu.rs

The convective heat transfer characteristics of any heat exchanger surface can be determined using the steady-state, periodic test and transient test techniques [2]. For a steady-state method, the temperatures of hot and cold fluids entering and leaving the heat exchanger, as well as flow rates are measured, and when steady state is achieved it is possible to determine heat flux, thus the overall heat transfer coefficient. In the transient technique method, after the steady-state is achieved, the temperature of the fluid entering the heat exchanger is suddenly changed. The heat transfer coefficient can be determined from temperature-time history data. The periodic test techniques represent a variation of the transient method in which the temperature of the fluid entering the heat exchanger is continuously varied.

The goal of this paper is to investigate thermal and fluid flow process at close to ambiental conditions on the air side of an air/water perforated plate heat exchanger, based on the steady-state method. The research was conducted in two directions: experimental research of the perforated plate package with one, two and three plates with constant porosity and an analytical research of the single plate with varied porosity.

2. Experimental setup

In this experiment, an MHE consisting of perforated plates with a porosity of 25,6%, 2 mm thick, with square arranged 2 mm in diameter perforations was tested. Each plate was divided into two sections: central section through which water flows and peripheral section, through which the air flows. Sections were separated by a gasket (fig. 1). The plates were placed in the channel of the experimental chamber, at which entrance was a thrust fan with the airflow from 100 to 300 m^3/h. The distance between the plates in the package was set to 5 mm in order to provide access for the measuring equipment (fig. 2).

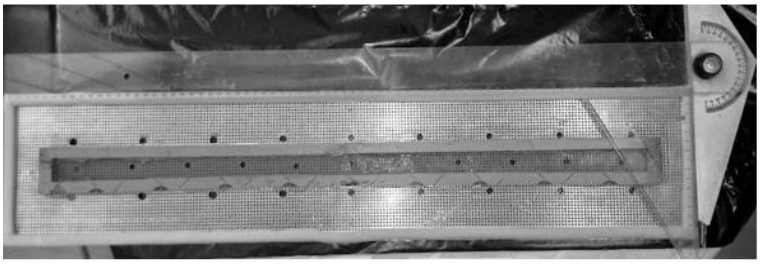

Figure 1. A perforated plate with a gasket

As a heating fluid, water was used, while the heat source was a boiler with adjustable power. Hot water enters the collector and flows through the central part of the plate. The heat is transferred from the water to the plate.

Exchanged heat is further transferred by conduction through the plate towards the edge of the plate, where it comes into the contact with the cooler air stream. The heat is then transferred by means of convection from the plate to the cooler air stream.

For the needs of the experiment, a measuring plate was set-up. The measuring plate consists of thermocouples, which were set on the perforated plate. In total 11 thermocouples were placed, 5 on each side of the plate (fig. 3) and one as control thermocouple for the error estimation. Heads of thermocouples were covered with thermally conductive paste in order to ensure thermal contact between thermocouples and plate. Thermocouples were calibrated before the experiment. Also, the temperatures of air at the inlet and the outlet of the chamber were measured by thermocouples.

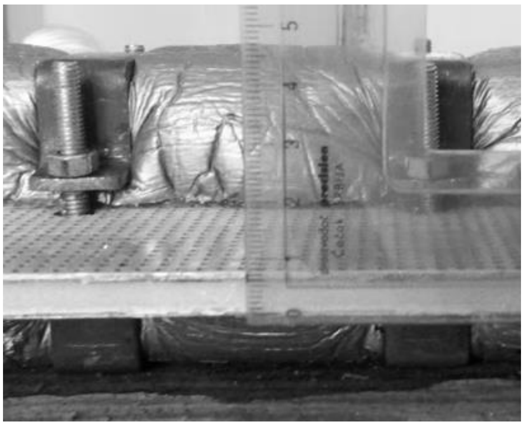

Figure 2. A package of two plates

The cold end of thermocouples was obtained as a mixture of water and ice. During each experiment, the air flow rate, water flow rate, temperatures at the inlet and outlet of the chamber, temperatures at the plate surface and temperatures of air between the plates were measured. The scheme of the experimental setup is presented in the fig. 4. During the experimental research the following assumptions were made:

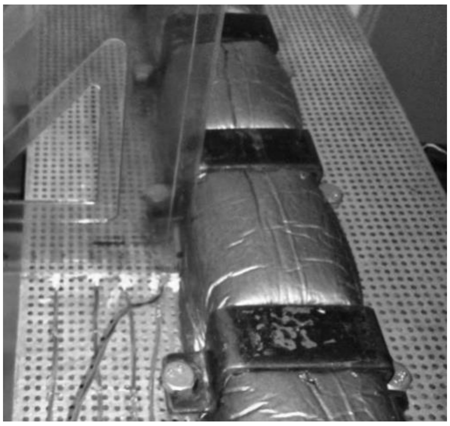

Figure 3. Thermocouples positions on the perforated plate

The scheme of the experimental setup is presented in the fig. 4. During the experimental research the following assumptions were made:

- The first plate in the package of two plates acts as the first plate in the package of two or more plates;
- The second plate in the package of two plates acts as the last plate in the package of two or more plates;
- The second plate in the package of three plates acts as any inner plate in the package of three or more plates.

According to these assumptions the packages of one, two and three plates were formed. The measurements were conducted when the thermal equilibrium was achieved, *i.e.* when the change of the water temperature was less than 0.1 K during 10 min period [4].

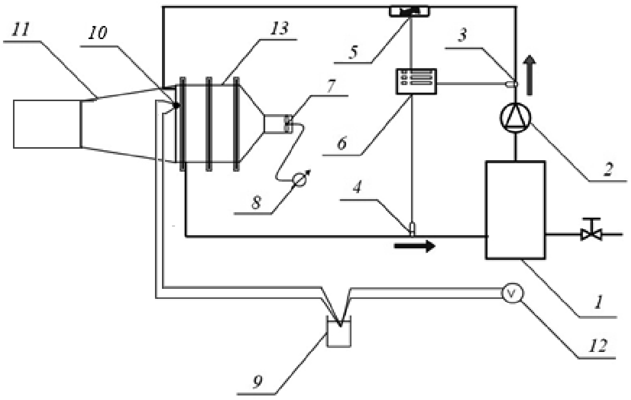

Figure 4. Experimental setup: 1 – boiler, 2 – pump, 3,4 – PT probes, 5 – ultrasonic water flow meter, 6 – acquisition unit, 7 – fan unit, 8 – fan speed control, 9 – cold end of thermocouples, 10 – thermocouples, 11 – Alnor balometer, 12 – millivoltmeter, 13 - chamber

After achieving the thermal equilibrium the following readings were done:

- Water flow rate;
- Water temperature at the inlet;
- Water temperature at the outlet;
- Air flow rate;
- Air temperature at the chamber inlet;
- Air temperature at the chamber outlet;
- Temperatures of the perforated plate.

According to the readings, the convective heat transfer rate $\dot{Q}_w$ from the water side is equal to

$$\dot{Q}_w = \rho_w \dot{V}_w c_w \Delta T_w \tag{1}$$

Similarly, the heat transfer rate of air side is equal to

$$\dot{Q}_L = \rho_L \dot{V}_L c_L \Delta T_L \tag{2}$$

The heat transfer rate for the perforated plate was calculated as the average value of water and air side as

$$\dot{Q}_{av} = \frac{\dot{Q}_L + \dot{Q}_w}{2} \tag{3}$$

and the measurement error is estimated as

$$\varepsilon = \frac{\sqrt{\left(\dot{Q}_L - \dot{Q}_{av}\right)^2 + \left(\dot{Q}_w - \dot{Q}_{av}\right)^2}}{\dot{Q}_{av}} \tag{4}$$

For the analysis, only measurements with the error less than 10% were used [5,6]. The overall heat transfer coefficient α is defined as

$$\alpha = \frac{\dot{Q}_{av}}{F\Delta\theta} \tag{5}$$

where *ΔΘ* is the difference between the average air temperature and the average temperature of perforated plates, while *F* is the overall heat exchanger surface on the air side. The partial heat transfer coefficients were determined on the basis of the air temperature difference on the upwind and downwind side of the observed plate and the average plate temperature

$$\alpha_{\mathrm{i}} = \frac{\dot{m}c_{\mathrm{L}}(t_{\mathrm{dow}} - t_{\mathrm{upw}})}{F\Delta\theta_{\mathrm{i}}} \tag{6}$$

where α_{i}represents the heat transfer coefficient for the i-th plate and $\Delta\theta_i$ represent the difference between the average plate temperature and the average air temperature. The obtained results for the individual heat transfer coefficients have been presented on the fig. 5.

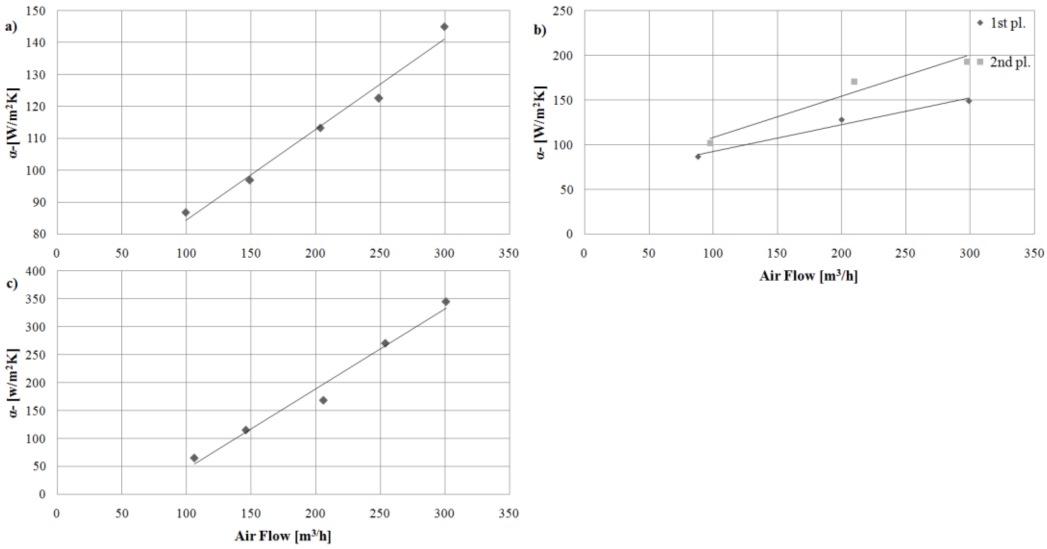

Fig. 5. Heat transfer coefficients on the air side for the a) one plate, b) the first and the second plate in the package of two plates, c) middle plate in the package of three plates

3. Numerical Setup

Three-dimensional steady-state turbulent flow is studied using the commercial software PHOENICS. The Reynolds Averaged Navier–Stokes equations (RANS) together with an eddy viscosity turbulence model are solved. In order to choose the best suitable model, several of *k*-*ε* variants were tested: standard *k*-*ε* model, low-RE *k*-*ε*, RNG *k*-*ε* and *k*-*ω* model. Although all of them gave similar results, the RNG *k*-*ε* model presented itself as the fastest converging, and therefore was adopted for the simulation. The advantage of RNG *k*-*ε* turbulence model stands for its advantage in resolving flow separation and generally better performance than the standard *k*-*ε* model and better treatment of flow for lower Reynolds numbers [7,8,9]. In general, the RNG *k*-*ε* model could be written in the form of a transport equation

$$\frac{\partial(\rho\Phi)}{\partial t} + \frac{\partial\left(\rho\Phi u_{\mathrm{j}}\right)}{\partial x_{\mathrm{i}}} = \frac{\partial}{\partial \mathrm{x_i}}\left(\frac{\partial \Gamma_{\Phi}}{\partial \mathrm{x_i}}\right) + S_{\Phi} \tag{7}$$

where the details have been presented in the tab. 1.

In order to model the local flow structure, a representative unit with 3x3 holes is defined (fig. 6). A uniform velocity is set at the inlet and a constant pressure boundary at the outlet. Turbulence quantities at the inlet are determined from the empirical correlations for turbulence intensity for internal pipe flows [8]. The domain is created as a sufficiently long (>20*d*) on the downstream side to ensure the simulation results.

Table 1. RNG *k*-*ε* turbulent model transport equations and constants

Transport equation	Φ	Γ_Φ	S_Φ
Turbulent kinetic energy	k	ν_t/σ_k	$\rho\ (G - \varepsilon)$
Turbulent kinetic energy dissipation	ε	ν_t/σ_ε	$\rho\ (\varepsilon / k)(C_{\varepsilon 1}G - C_{\varepsilon 2}\varepsilon)$
$G = \nu_t\ (\partial_k U_i + \partial_i U_k)\ \partial_k U_i$			$\nu_t = C_\mu k^2 / \varepsilon$
$(\sigma_k, \sigma_\varepsilon, C_{\varepsilon 1}, C_{\varepsilon 2}, C_\mu) = (0.7194,\ 0.7194,\ 1.42,\ 1.68,\ 0.0845)$			

In order to generate the optimal grid the grid independence test was done. The grid size was varied in two directions along the plate length and width, regarding the Y-Z plane (fig. 6). The grid was set to square in the Y-Z plane, and the length of the cell in these two directions was varied from 0.88 to 0.2 mm, while the fluid temperature at the outlet was chosen as a quality parameter. The results showed that under the cell size of 0.8 mm, the temperature at the outlet was varying not more than 0.1 K (tab. 2.) [7].

Table 2. Temperature variation at the outlet

Cell size [mm]	0.88	0.8	0.72	0.6	0.53	0.35	0.26
Out. temp. [°C]	21.65	22.3	22.28	22.33	22.35	22.22	22.4

According to this, the cell length was chosen to be 0.5 mm, *i.e.* minimum 4 cells per hole diameter. The grid in the flow direction was refined near solid walls so that y^+ was less than 30 and the standard wall functions could be applied. The air velocity and the temperature at the inlet, as well as the constant temperature boundary conditions on the plate surface, have been set according to the earlier experimental research [8,10,11]. A typical convergence of the numerical research has been presented in the fig. 6, and typical results are presented in the fig. 7.

Similarly to the eq. (1) and (2) energy balance for the fluid side is represented as:

$$\dot{\mathrm{Q}} = \rho w A c_{\mathrm{L}}(t_{\mathrm{out}} - \mathrm{t}_{\mathrm{in}}), \tag{8}$$

where c_p represents mass specific heat capacity, *A* cross-section area and *w* is the fluid velocity. On the other hand the heat transmitted from the plate is equal to:

$$\dot{Q} = \alpha F\left(t_{\mathrm{pl}} - t_{\mathrm{L}}\right), \tag{9}$$

where *F* represents the active heat transfer surface. Combining eq. (8) and (9), heat transfer coefficient is then equal to:

$$\alpha = \frac{\rho w A c_{\mathrm{L}}(t_{\mathrm{out}} - t_{\mathrm{in}})}{F(t_{\mathrm{pl}} - t_{\mathrm{L}})}. \tag{10}$$

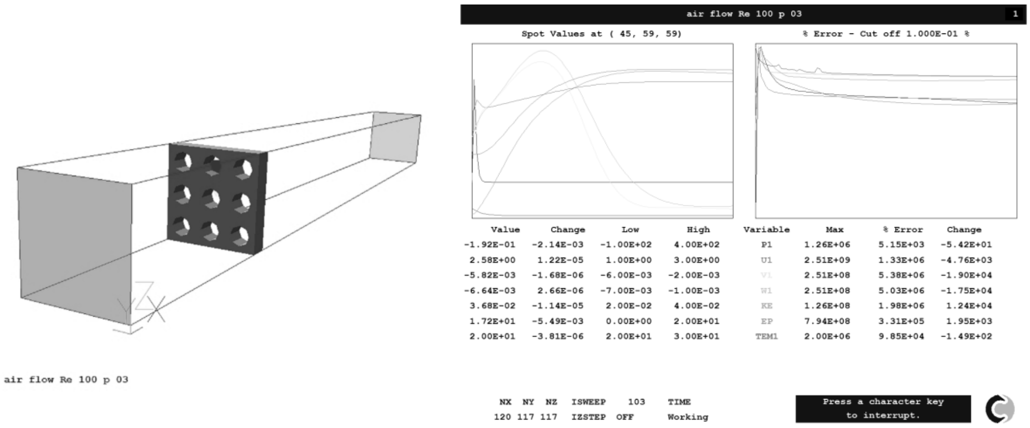

Fig. 6. A numerical model of the perforated plate (left) and a typical convergence of the numerical simulation (right)

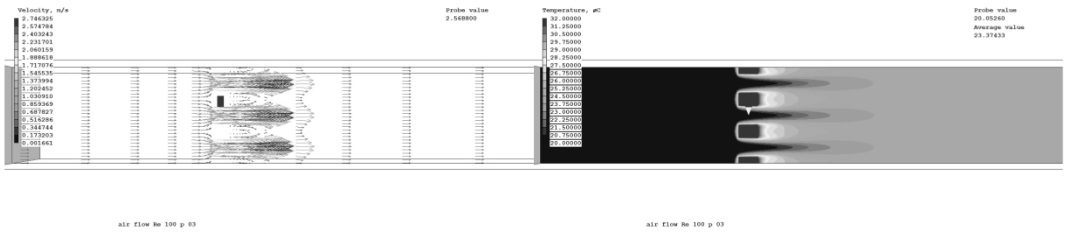

Fig. 7. An example of velocity field (left) and temperature field (right)

4. Results and discussion

For the Nusselt criteria an arbitrary function was chosen in the following form

$$\mathrm{Nu} = \mathrm{C}\left(\frac{p}{d}\right)^{\mathrm{m}} \mathrm{Re}^{\mathrm{n}}, \tag{11}$$

according to earlier research of the Kutcher [12]. The term *p/d* of eq. (11) on the right-hand side is inverse proportional to the square root of the porosity and therefore represents the influence of the porosity on the heat transfer. The Reynolds number is defined in the function of free-stream fluid velocity *w*

$$\mathrm{Re} = \frac{wp}{\nu}, \tag{12}$$

and the Nusselt number is equal to

$$\mathrm{Nu} = \frac{\alpha p}{\lambda}, \tag{13}$$

The characteristic length in Reynolds and Nusselt number *p* represents the size of the pitch between holes. The best fitting results for the single plate were found at

$$\mathrm{Nu} = 0.803\left(\frac{p}{d}\right)^{0.492} \mathrm{Re}^{0.524}, \tag{14}$$

for $50 \leq \mathrm{Re} \leq 500$ with regression of 0.97. Since the Prandtl number of air for testing conditions is equal to 0.71, the Nusselt criteria for gases could be written in the form

$$\mathrm{Nu} = 0.900\left(\frac{p}{d}\right)^{0.492} \mathrm{Re}^{0.524}\mathrm{Pr}^{0.333}, \tag{15}$$

The comparison of results obtained by numerical research and measurements is presented on the fig. 8 and 9.

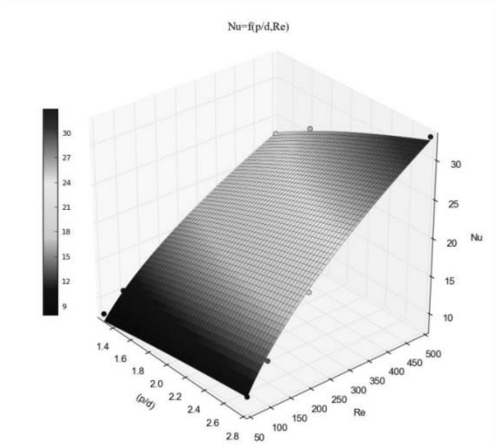

Fig. 8. Nusselt criteria as the function of geometry parameters and Reynolds number

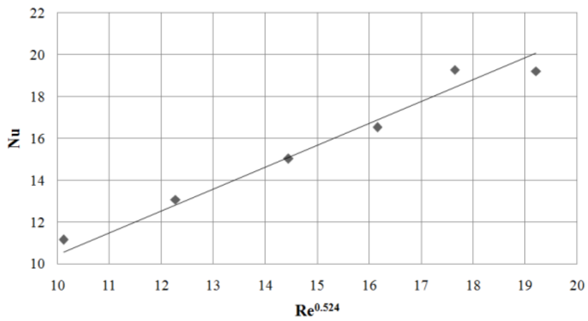

Fig. 9. Comparison with measurements (right)

Further, the influence of the number of plates on the Nusselt number is assumed to be in the form

$$\mathrm{Nu_{pack}} = N\mathrm{Nu} \tag{16}$$

where N represents the influence of plate numbers and $\mathrm{Nu_{pack}}$ represents the Nusselt number of the package of perforated plates. The best fitting has been obtained from the function in the form

$$N = 1.02n^{\left(0.56+\frac{51.36}{\mathrm{Re}}\right)} \tag{17}$$

The research has shown that for the packages of five and more plates the heat transfer coefficient becomes a constant, and as it could be expected tends to the value of the heat transfer coefficient of the middle plate [13].

5. Conclusions

The goal of this research was to investigate the heat transfer process of matrix heat exchangers on the air side, at the close to ambient conditions. The research was conducted in two directions - experimental research and CFD research. The results have showed that the convective heat transfer for a matrix heat exchanger depends strongly on geometry parameters - the plate porosity and partly on the number of plates. Further, a Nusselt criteria equation was derived as the function of geometry parameters, Reynolds number, Prandtl number and a number of plates. On the end, the comparison of experimental results against obtained criteria equations was done and it has showed a good agreement.

Acknowledgments

The research presented in this paper is part of research done within the project III 42008 supported by the Ministry of Education, Science, and Technological Development of the Republic of Serbia and College of Applied Technical Sciences in Niš. Also, the authors would like to express their gratitude to Mr. Milivoj Pejin and Mr. Branko Babić for their contribution to the research.

Nomenclature

c	- heat capacity, [$Jkg^{-1}K^{-1}$]
d	- perforation diameter, [mm]
F	- heat transfer area, [m^2]
k	- kinetic energy of turbulence, [m^2s^{-2}]
$\dot{m}$	- mass flow rate, [$kg\ s^{-1}$]
N	- function of number of plates, [-]
n	- number of plates, [-]
p	- pitch, [mm]
$\dot{Q}$	- heat flux, [W]
t	- temperature, [°C]
$\dot{V}$	- volume flow rate, [$m^3\ s^{-2}$]
w	- fluid velocity, [$m\ s^{-1}$]
Greek symbols	
α	- heat transfer coefficient, [$Wm^{-2}K^{-1}$]
ε	- dissipation of kinetic energy of turbulence, [m^2s^{-3}]
ρ	- fluid density, [kgm^{-3}]
Subscripts	
av	- average
dow	- downwind
i	- coordinate
in	- inlet
out	- outlet
L	- air
up	- upwind
w	- water

References

[1] McMahon, H. O., Bowen, R. J., Bleye, Jr., G. A., A Perforated Plate Heat Exchanger, *Trans ASME*, *72* (1950), pp. 623-632

[2] Krishnakumar, K., Venkataratham, G., Transient Testing of Perforated Plate Matrix Heat Exchangers, *Cryogenics*, *43* (2003), 2, pp. 101-109

[3] Venkataratham, G., Sarangi, S., Matrix Heat Exchangers and their Application in Cryogenic System, *Cryogenics*, *30* (1990), pp. 907-918

[4] Bukurov, M., Bikić, S., Ilin, S., Đurđević, M., Dragutinović, G., Heat Exchangers with Perforated Plates, *Journal on Processing and Energy in Agriculture*, *15* (2011), pp. 179-182

[5] Glažar, V., Optimization of compact heat exchanger geometry (in Croatian), Ph. D. thesis, University of Rijeka, Rijeka, Croatia, 2011

[6] Vukić M., Experimental and numerical investigation of thermal and fluid flow processes in in shell-and-tube heat exchangers (in Serbian), Ph. D. thesis, University of Niš, Niš, Serbia, 2004

[7] Tomić, M. A., Živković, P. M., Vukić, M. V., Ilić, G. S., Stojiljković, M. M., Numerical study of perforated plate convective heat transfer, *Thermal Science*, *18* (2014), 3, pp. 949-956

[8] Tomić, M., Experimental and Numerical research of Thermal and Flow Process in the Package of Perforated Plates (in Serbian), Ph. D. thesis, University of Niš, Niš, Serbia, 2015

[9] ***, Concentration Heat and Momentum Ltd, http://www.cham.co.uk/

[10] Tomić, M., Vukić, M., Živković, P., Stevanović, Ž., Experimental investigation of thermal and fluid flow processes in a perforated plate heat exchanger, *Acta Technica Corvininesis - Bulletin of Engineering*, *9* (2016), 1, pp. 117-120

[11] Tomić, M., Živković, P., Vukić, M., Ilić G., Ayed S., The methodology for determination of perforated plate heat transfer coefficient. In: Stefanović P., Cvetinović D., Bakić V., editors. Proceedings of the Powerplants 2014; 2014 28-31 October; Zlatibor, Serbia. Society of Thermal Engineers of Serbia:90.

[12] Kutscher, C. F., An Investigation of Heat Transfer For Air Flow Through Low Porosity Perforated Plates, Ph. D. thesis, Boulder, USA University of Colorado at Boulder, Boulder, 1992

[13] Tomić, A., Živković, P., Vukić, M., Stevanović, Ž., Milutinović, B., Experimental and Analytical Research of the Heat Transfer Process in the Package of Perforated Plates, *Proceedings*,. (Mitrović, D., Laković, M., Stojiljković, M., Ignjatović M., editors), 17th Symposium on Thermal Science and Engineering of Serbia - SIMTERM 2015, Sokobanja, Serbia, 2015, pp. 97-104.